ELSEVIER

Applied Catalysis A: General 167 (1998) 183–193

APPLIED CATALYSIS A: GENERAL

Use of aluminophosphate molecular sieves in CO hydrogenation

M. Luisa Cubeiro[a,*], Carmen M. López[a], Alicia Colmenares[a], Luisa Teixeira[a], Mireya R. Goldwasser[a], M. Josefina Pérez-Zurita[a], Francisco Machado[a], Fernando González-Jiménez[a,b]

[a] *Centro de Catálisis Petróleo y Petroquímica, Universidad Central de Venezuela, Facultad de Ciencias, Escuela de Química, A.P. 47102, Los Chaguaramos, Caracas 1020-A, Venezuela*

[b] *Universidad Central de Venezuela, Facultad de Ciencias, Escuela de Física, Los Chaguaramos, Caracas 1020-A, Venezuela*

Received 4 September 1997; received in revised form 26 September 1997; accepted 4 October 1997

Abstract

The behaviour in syngas conversion of Me/$AlPO_4$-5 and MeAPO-5 (Me=Fe, Co, ~4 wt%), as well as that of hybrid systems comprising an iron Fischer–Tropsch (FT) catalyst physically mixed with SAPO-5, FAPO-5, SAPO-11 and FAPO-11, was studied at 1.2 MPa, 573 K and $H_2/CO=1$. Conversion of CO was much lower for Fe/$AlPO_4$-5 and MeAPOs than for Co/$AlPO_4$-5, which could be related to the presence of the metal in high-oxidation states on the former. Significant differences in selectivity were observed as a result of changes in the type of metal and in the way that the metal is introduced in the catalyst (added to the synthesis gel or impregnated on the molecular sieve). These differences in selectivity were explained in terms of the facility of forming alkenes (related to metal sites) and the presence of acid sites. Alkenes formed on the FT catalyst underwent oligomerisation, cracking, skeletal isomerisation and hydrogen transfer reactions in the presence of the physically mixed SAPO-5 and FAPO-5. Double bond shift and skeletal isomerisation were the only alkene transformations observed on the mixtures of FT with AEL-like catalysts (FT-FAPO-11 and FT-SAPO-11). Deactivation of acid sites with time-on-stream was evidenced for the physical FT-molecular sieves mixtures. However, their higher selectivity toward light hydrocarbons, as compared to that in the absence of molecular sieves, persisted. It was observed that the FAPO phase (FAPO-5 or FAPO-11) added to the FT catalyst led to an increase in the syngas conversion, probably due to the participation of iron-species associated with the molecular sieves. © 1998 Elsevier Science B.V.

Keywords: Syngas conversion; Fischer–Tropsch synthesis; Carbon monoxide hydrogenation; FAPO; SAPO; CoAPO; $AlPO_4$-5; MeAPO; AFI; AEL

1. Introduction

The Fischer–Tropsch (FT) synthesis emerges as a promising option to obtain clean fuels and chemical products from natural gas and coal due to environmental restrictions and the decrease of petroleum reserves. Proper selection of the catalyst and of the reaction conditions allow changes in product distribution. However, as a result of the chain growth mechanism, there is inherent limitations to the changes in selectivity. Due to their properties, i.e. high-surface area, acidity and shape selectivity molecular sieves have attracted attention for their application on the FT synthesis in several ways [1,2]. Their use as supports has been considered not only to provide high metal

*Corresponding author. Fax: (+58-2)605.21.36; e-mail: mcubeiro@strix.ciens.ucv.ve

PII S0926-860X(97)00300-1

dispersions, but also to take advantage on possible shape selectivity effects [1,3]. It has also been proposed that unusual selectivities could be obtained when the metal (Fe, Co) is incorporated into the molecular sieve framework [2,4,5]. The effect of the acidity of zeolites on the FT synthesis has also been tested. The zeolitic phase has been used either as support or physically mixed with the FT catalyst or in a separated bed. In this way, the acidic–zeolitic phase can intercept and convert linear 1-alkenes produced by the FT component. For instance, Y type [6] and ZSM-5 [2] zeolites have been used to provide gasoline-range products of enhanced octane ratings. Aluminophosphate molecular sieves can be prepared over a wide range of framework composition and crystalline topology. So these structures look very attractive for FT synthesis. Surprisingly they have been scarcely studied for this reaction.

$AlPO_4$-5 (AFI) and $AlPO_4$-11 (AEL) molecular sieves have one-dimensional channel system with large (~0.8 nm) and medium (~0.6 nm) pores, respectively. The acid properties of these solids can be modified by introducing elements different from Al and P in the framework at different loading. Appropriated combination of both acidity and crystal topology can made these structures very active and selective for the transformation of linear alkenes into branched alkenes. Thus, AEL-based catalysts have been shown to be very selective toward the skeletal rearrangement during the transformation of 1-butene [7].

In the present study, the catalytic behaviour in syngas conversion of iron- and cobalt-aluminophosphates with the AFI structure (FAPO-5, CoAPO-5) was compared to that of the same metals supported on $AlPO_4$-5 (Me/$AlPO_4$-5). Bifunctional systems, comprising an iron-promoted FT catalyst physically mixed with aluminophosphate molecular sieves (FAPO-5, SAPO-5, FAPO-11 and SAPO-11) were also investigated.

2. Experimental

2.1. Catalysts preparation

The FAPO-5, CoAPO-5, $AlPO_4$-5, SAPO-5, FAPO-11 and SAPO-11 molecular sieves were synthesised according to the procedures given in Refs. [8–12]. In Table 1 synthesis conditions are presented. After washing and drying, the solids were calcined under an air flow (20 ml/min g) at 473 K for 1 h. Then, the temperature was raised to 813 K and kept there for 16 h. Me/$AlPO_4$-5 were prepared by incipient wetness impregnation of $AlPO_4$-5 with iron-III and cobalt-II nitrates, followed by drying at 413 K and calcination in air flow (20 ml/min g) at 723 K for 3 h. The FeKMn/Al_2O_3 FT catalyst was obtained by co-impregnation of iron nitrate and the promoter salts (manganese nitrate and potassium carbonate) on Kentjen CK-300 γ-Al_2O_3 (particle size<0.12 mm). Drying and calcination were as for Me/$AlPO_4$-5 solids.

The FT catalyst was physically mixed with quartz sand as diluent (FTQ) or with FAPO-5 (FTF-5), SAPO-5 (FTS-5), FAPO-11 (FTF-11) or SAPO-11 (FTS-11). The FT : diluent or sieve proportion was 1 : 1 (wt : wt).

2.2. Catalysts characterisation

X-ray diffraction (XRD) patterns of the aluminophosphate molecular sieves were obtained using a

Table 1
Conditions for aluminophosphates synthesis

Solid	Gel molar composition	T_c (K)	t_c (h)
$AlPO_4$-5	$Al_2O_3 : P_2O_5 : TEAOH : 40H_2O$	423	24
SAPO-5	$Al_2O_3 : P_2O_5 : 1.5Et_3N : 0.4SiO_2 : 40H_2O$	473	24
FAPO-5	$0.9Al_2O_3 : P_2O_5 : 1.5Et_3N : 0.2FeO : 40H_2O$	423	24
CoAPO-5	$0.9Al_2O_3 : P_2O_5 : 1.5Et_3N : 0.05CoO : 40H_2O$	473	28
FAPO-11	$0.9Al_2O_3 : P_2O_5 : DPA : 0.2FeO : 40H_2O$	423	48
SAPO-11	$Al_2O_3 : P_2O_5 : 0.3SiO_2 : DPA : 50H_2O$	473	24

TEAOH: tethraetylammonium hydroxide; Et_3N: thriethylamine; DPA: dipropylamine; T_c and t_c: crystallisation temperature and time, respectively.

Philips diffractometer with CoK_α radiation. Surface areas were measured by nitrogen adsorption with a Micromeritics Flowsorb II 2300 analyser. Elemental analysis of the solids was performed by ICP (argon plasma) and flame absorption and emission, with Jobin Yvon JY24 and Varian Techtron spectrophotometers, respectively. ^{29}Si MAS NMR spectra were recorded in a Bruker AM spectrometer, following reference [10]. Bulk iron phases of FAPOs were analysed by ^{57}Fe Mössbauer spectroscopy, using a source of ^{57}Co in a Pd matrix. About 0.2–0.3 g of the sample was placed in an aluminium holder and sealed with epoxy. Spectra were recorded at room temperature and fitted by means of a least-squares fitting program.

2.3. CO hydrogenation reaction

The CO hydrogenation reaction was performed in a continuous-flow system with a fixed-bed stainless steel reactor (1.07 cm ID). Liquid products were collected in a stainless steel trap at room temperature. Before reaction FAPO-5, Fe/$AlPO_4$-5, as well as the physically mixed iron FT catalyst were submitted to reduction (H_2, 50 ml/min g, 723 K, 16 h) followed by carburisation (CO, 25 ml/min g, 423 K, 4 h, 573 K, 17 h). Pre-treatment conditions were the same for cobalt catalysts, but the carburisation step was omitted. Catalytic tests were performed, using ~3 g of the pre-treated solid, at 573 K and 1.2 MPa, (H_2/CO=1). Space velocities expressed as litres of the feed gas per gram of catalyst per hour were 0.6 l/g_{cat} h for MeAPOs and Me/$AlPO_4$-5 and 1.2 l/$g_{FT\ cat}$ h for the FT catalyst physically mixed with quartz sand or molecular sieves. For the physical mixtures, the weight of catalyst was taken to be that of the FT catalyst alone. Runs were carried out over a period of 24 h on stream for the MeAPOs and Me/$AlPO_4$-5, and between 48 and 96 h for the composite catalysts. Effluent gases were analysed periodically by gas chromatography. Permanent gases (N_2, CO, CH_4, CO_2) were analysed on line with a Varian 3300 gas chromatograph provided with a thermal conductivity detector using a Carbosieve SII packed column. C_1–C_7 hydrocarbons were analysed in a Chrompack CP 9001 chromatograph with a flame ionisation detector and a WCOT Al_2O_3/KCl fused silica column. CO conversions were determined using nitrogen, present in the feed gas (5%) as internal standard, and chromatograms were correlated through methane. Hydrocarbon distributions for MeAPOs and Me/$AlPO_4$-5 are presented as C_n/C_3 ratios. Because of the low syngas conversion obtained in some cases, detection of C_{4+} hydrocarbons was difficult. For tests with the physically mixed FT catalyst selectivities were determined as: carbon converted to a given product/total carbon converted. CO_2 free selectivities were obtained as the ratio: selectivity to a hydrocarbon fraction /(1-CO_2 selectivity). The C_{8+} selectivity was obtained as the difference between 100% and the C_1–C_7 hydrocarbons selectivity. It includes, besides the C_{8+} hydrocarbons, oxygenates that could be formed by the FT catalyst.

3. Results and discussion

3.1. Catalysts characterisation

The XRD patterns of the as synthesised solids all showed the AFI or AEL structures as the only crystalline phases (Fig. 1). The cobalt and iron contents of aluminophosphates-based catalysts were 3–4 wt%, except for CoAPO-5 (Table 2), since the preparation of this solid was only possible at a lower cobalt loading (1.2 wt%). A cobalt-containing synthesis gel, prepared with the same metal loading and under conditions similar to those used in the FAPO-5 synthesis, led to a high purity CoAPO-34 solid having the TO_2 formula given in Table 2. This solid was also tested for syngas conversion.

According to the elemental analysis (TO_2 formulas, Table 2) substitution of aluminium by iron or cobalt for FAPO-5 and CoAPO-5 seemed to occur. However, for CoAPO-34 the ratio P/(Al+Co) was lower than unity, suggesting the occurrence of extra-framework cobalt. ^{29}Si MAS NMR spectrum for SAPO-5 (Fig. 2a) showed a signal at around −90 ppm typical of a Si(4Al) environment, suggesting the incorporation of silicon mainly by the SM2 mechanism. By contrast, for SAPO-11 (Fig. 2b) a signal at −113 ppm, associated to Si(0Al), was observed, indicating the presence of 'silicon islands' in the solid. Pyridine adsorption followed by FTIR showed a higher number of Brönsted acid sites for SAPO-5 than for SAPO-11 [10]. For SAPO-5, a significant proportion of acid sites (60%) did not retain pyridine at temperatures higher

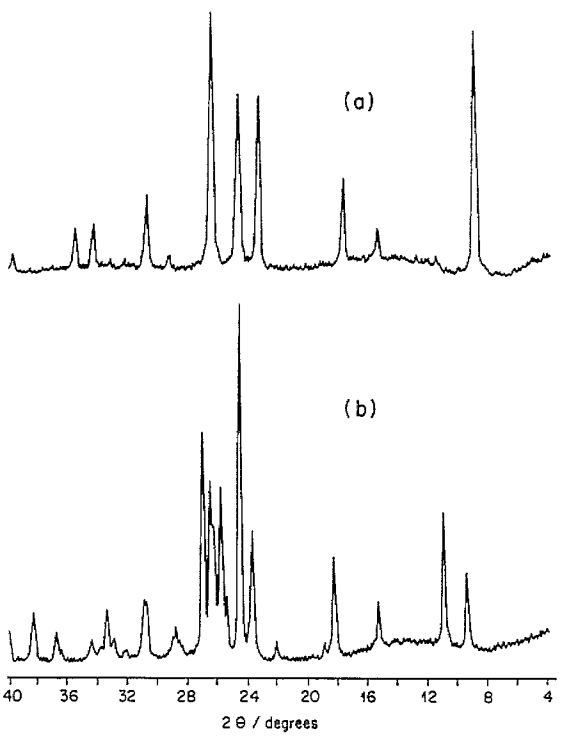

Fig. 1. XRD patterns of as synthesised (a) FAPO-5; and (b) FAPO-11.

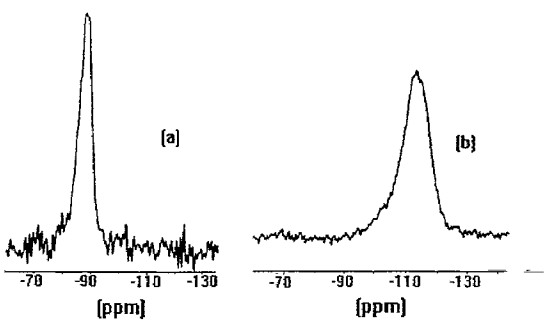

Fig. 2. ^{29}Si MAS NMR of (a) SAPO-5; and (b) SAPO-11.

than 623 K. For SAPO-11, however, nearly 100% of the acid sites retained pyridine at temperatures higher than 623 K.

Impregnation of $AlPO_4$-5 with iron led to a significant loss of surface area, whereas the decrease in sorption capacity by cobalt impregnation was much less (Table 2). A larger decrease of the XRD peaks intensity relative to that of the support was also observed for Fe/$AlPO_4$-5 (close to 60%). This concomitant loss of N_2 sorption capacity and XRD crystallinity strongly suggests structural modification of the molecular sieve as a result of the impregnation procedure. In fact, the high acidity of the impregnating solution due to the iron hydrolysis might have caused a partial crystalline collapse.

The structure of CoAPO-34 is of the chabazite type (CHA), this solid showed a very low-surface area (Table 2). A significant decrease (70%) of the XRD peaks intensity after calcination was detected. This is probably due to a partial crystalline collapse induced by the relatively high level of cobalt in the $AlPO_4$-34 framework.

The colour of the cobalt based solids suggested the existence of different oxidation states and co-ordination. The colour of CoAPOs changed from blue

Table 2
Elemental analysis and BET surface areas of calcined aluminophosphate molecular sieves and FT catalyst

Sample	TO_2 formula	Me (wt %)	S (m^2/g)
$AlPO_4$-5	$(P_{0.49}Al_{0.51})O_2$		358
Fe/$AlPO_4$-5	—	4.41	118
Co/$AlPO_4$-5	—	3.94	308
FAPO-5[a]	$(P_{0.51}Al_{0.43}Fe_{0.06})O_2$	3.68	306
CoAPO-5	$(P_{0.52}Al_{0.46}Co_{0.02})O_2$	1.18	400
CoAPO-34	$(P_{0.45}Al_{0.47}Co_{0.08})O_2$	5.64	36
FAPO-5[b]	$(P_{0.48}Al_{0.47}Fe_{0.05})O_2$	3.19	346
FAPO-11	$(P_{0.50}Al_{0.46}Fe_{0.04})O_2$	2.99	176
SAPO-5	$(P_{0.49}Al_{0.43}Si_{0.08})O_2$		323
SAPO-11	$(P_{0.47}Al_{0.47}Si_{0.06})O_2$		124
FeKMn/Al_2O_3	—	Fe: 19 (K: 5, Mn: 4)	144

[a] Used in MeAPOs tests.
[b] Used in FTF-5 mixture.

Table 3
Mössbauer parameters for FAPO-5 and Fe/$AlPO_4$-5

Solid	IS (mm/s)	FWHM (mm/s)	QS (mm/s)	Area (%)	Species
FAPO-5	0.38	0.70	1.06	91	Fe^{3+}
Calcined	1.20	0.50	2.02	9	Fe^{2+}
FAPO-5	0.40	0.70	0.61	58	Fe^{3+}
Red.–carb.	1.08	0.60	2.32	42	Fe^{2+}
FAPO-5	0.29	0.70	0.74	46	Fe^{3+}
After reaction	1.17	0.60	2.20	54	Fe^{2+}
Fe/$AlPO_4$-5	0.35	0.70	1.04	81	Fe^{3+}
Red.	0.74	0.60	1.31	19	Fe^{2+}
Fe/$AlPO_4$-5	0.14	0.50	0.40	12	SP[a]
Red.–carb.	1.14	0.60	2.19	88	Fe^{2+}
Fe/$AlPO_4$-5	0.14	0.50	0.35	10	SP[a]
After reaction	1.15	0.60	2.18	90	Fe^{2+}

IS: isomer shift, FWHM: full width at half maximum, QS: quadrupole splitting.
[a] Superparamagnetic species of iron carbides are probable.

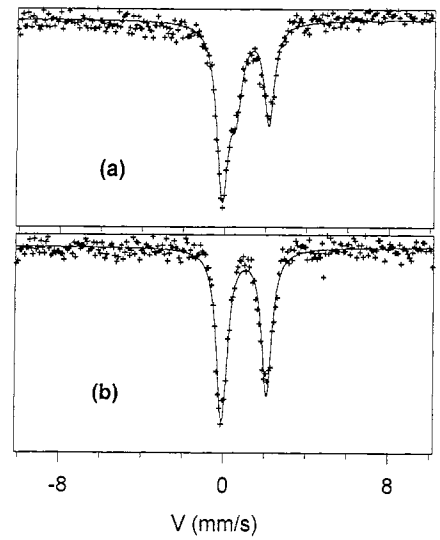

Fig. 3. Mössbauer spectra of (a) FAPO-5; and (b) Fe/$AlPO_4$-5 after reaction.

(tetrahedral Co^{2+}) for the as synthesised solids, to green after calcination (tetrahedral Co^{3+}) and again to blue after reduction (darker colours for CoAPO-34, with a higher cobalt content than CoAPO-5). On the other hand, Co/$AlPO_4$-5 was pink (octahedral Co^{2+}) after impregnation, and grey after calcination (probably due to cobalt oxide) and after reduction (probably due to zero valent cobalt).

The absence of magnetic signals in the Mössbauer spectrum of the calcined FAPO-5 indicated the presence of highly dispersed iron, which could be due to iron in the framework and/or iron in small superparamagnetic particles of extra-framework iron oxide. During the reduction and carburisation pre-treatment, and to a lesser extent under syngas reaction, nearly half of the Fe^{3+} was transformed to Fe^{2+} (Table 3, Fig. 3a). For Fe/$AlPO_4$-5 a progressive increase in the Fe^{2+} proportion after reduction with H_2 and mainly after CO treatment occurred (Table 3). After reaction (Fig. 3b), the iron-phase composition was unchanged, with about 10% of iron present as carbides. The transformation to metallic iron or carbides seems to be difficult for this catalyst. Similar results were reported previously for iron impregnated on $AlPO_4$-5 [13]. The formation of an iron compound by reaction with the support cannot be excluded, considering the reduction behaviour of iron in this catalyst and the changes in surface area and crystallinity.

3.2. CO hydrogenation reaction

3.2.1. MeAPOs and Me/$AlPO_4$-5

Co/$AlPO_4$-5 gave rise to 42% CO conversion, but the other catalysts showed very low activities (3% or lower). These results could be attributed to the transformation of cobalt to zero valent metal in Co/$AlPO_4$-5, whereas the metal was in the ionic states for the other solids, as shown by Mössbauer spectra for the iron catalysts and as suggested by the colour of the cobalt catalysts. Jong and Cheng [14] have found that for cobalt containing ZSM-5 zeolites, the catalytic activity in CO hydrogenation was directly proportional to the amount of metallic cobalt present.

The product selectivities of the cobalt catalysts showed great differences. Fig. 4 shows the C_n/C_3 ratios for Co/$AlPO_4$-5 and CoAPOs. The hydrocarbon distribution, referred to the C_3 fraction, indicates a much higher-methane formation for Co/$AlPO_4$-5 compared to CoAPOs. It is worth mentioning that the reaction temperature (573 K) chosen for comparative purposes is substantially higher than those commonly used with cobalt supported catalysts (450–520 K).

The alkenes/alkanes ratios for the C_2 and C_3 fractions (Fig. 5) indicated a higher alkenes selectivity for iron in comparison with cobalt catalysts. Generally,

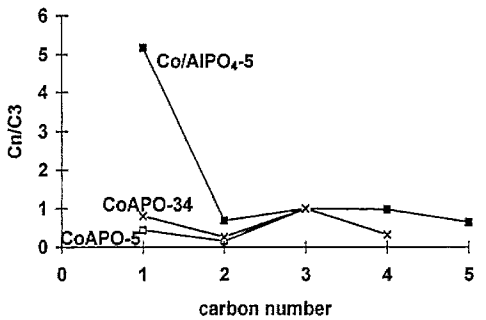

Fig. 4. Hydrocarbon distribution for CO hydrogenation on Co/$AlPO_4$-5 and CoAPOs (573 K, 1.2 MPa, $H_2/CO=1$, 0.6 l/g_{cat} h, 15 h on stream).

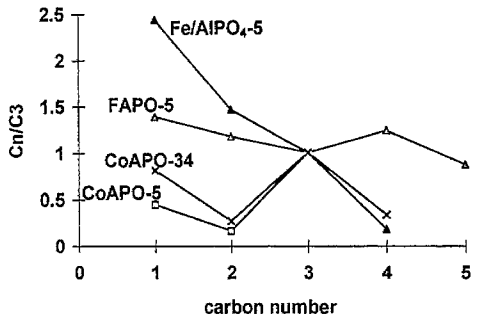

Fig. 6. Hydrocarbon distribution for CO hydrogenation on Fe/$AlPO_4$-5 and MeAPOs (573 K, 1.2 MPa, $H_2/CO=1$, 0.6 l/g_{cat} h, 15 h on stream).

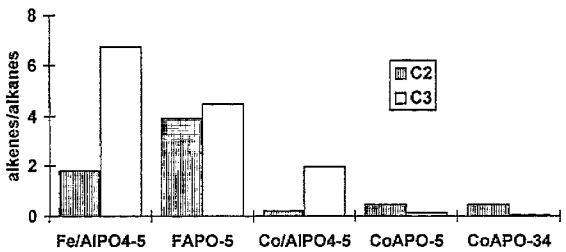

Fig. 5. Alkenes/alkanes ratios of the C_2 and C_3 fractions for CO hydrogenation on Me/$AlPO_4$-5 and MeAPOs (573 K, 1.2 MPa, $H_2/CO=1$, 0.6 l/g_{cat} h, 15 h on stream).

cobalt is a more active hydrogenation catalyst than iron. However, the difference in conversions must be taken into account when comparing Co/$AlPO_4$-5 with the other catalysts due to the probability of secondary alkenes hydrogenation. At lower CO conversions a higher alkenes selectivity should be expected.

FAPO-5 showed a higher ethylene/ethane ratio than Fe/$AlPO_4$-5, but the propylene/propane (Fig. 5), as well as the C_3/C_4 ratio (Fig. 6) were lower. This behaviour could be attributed to the transformation of propylene into other hydrocarbons by oligomerisation and subsequent cracking of oligomers on the acid sites of FAPO-5 [15].

CoAPO-34 and CoAPO-5 showed a low ethylene/ethane ratio and the lowest propylene/propane ratio among all the catalysts (Fig. 5). Since a well defined maximum on the C_3 fraction was observed (Fig. 6), it seems that propylene was hardly formed on CoAPOs. The species responsible for CO hydrogenation in CoAPOs appears to have a high selectivity to alkanes formation. Acidity was not evident from CoAPOs selectivity in syngas conversion.

Linear hydrocarbons are the main products over conventional FT catalysts. Among all catalysts only FAPO-5 and Co/$AlPO_4$-5 gave rise to significant amounts of branched hydrocarbons. After 15 h on stream FAPO-5 showed 56% of iso-butane on C_4 hydrocarbons and 62% of iso-pentane on the C_5 fraction. For Co/$AlPO_4$-5 the proportions were 27 and 49%, respectively. With FAPO-5 iso-alkanes could be produced through skeletal isomerisation of alkenes and hydrogen transfer reactions on the acid sites [6]. With Co/$AlPO_4$-5, at a higher syngas conversion, iso-alkanes could be produced by secondary reactions on the cobalt metal site; however a contribution of the support acidity cannot be discarded.

The notable differences observed in activity and selectivity among MeAPOs and Me/$AlPO_4$-5 can be related to different oxidation states of the metal (cobalt catalysts), different alkenes selectivity (CoAPOs and FAPO-5) and different acidity (FAPO-5 and Fe/$AlPO_4$-5).

3.2.2. *Mixtures with iron FT catalyst*

The use of aluminophosphate molecular sieves as acidic components in bifunctional systems is another possible application to the FT synthesis. An iron catalyst (19% of Fe, Table 2) promoted with potassium and manganese, with high alkenes selectivity, was used as FT component. FAPO-5, SAPO-5, FAPO-11 and SAPO-11 were the acidic components.

Fig. 7 shows the CO conversion as a function of time-on-stream for the FT catalyst physically mixed

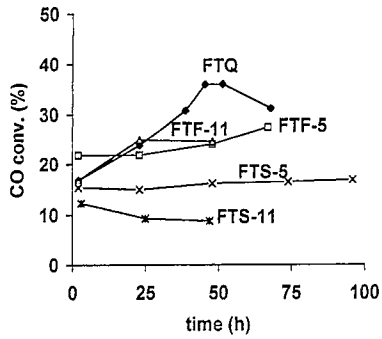

Fig. 7. CO conversion vs. time-on-stream for the FT catalyst physically mixed with quartz sand and with AFI and AEL molecular sieves (573 K, 1.2 MPa, $H_2/CO=1$, 1.2 l/g_{FT} h, FT : quartz sand or molecular sieve 1 : 1).

with quartz sand and with AFI and AEL molecular sieves. For the FT catalyst mixed with quartz sand (FTQ) a maximum in CO conversion with time-on-stream was observed. It was stated previously that the behaviour of iron catalysts is strongly dependent on preparation, pre-treatment, as well as on reaction conditions [16,17]. Since the carburisation of the catalyst was not complete after the pre-treatment, as indicated by the Mössbauer spectra, the initial increase in activity could be due to a continuation of iron transformation under the syngas. The subsequent deactivation observed was probably due to deposition of carbon and high-molecular weight hydrocarbons and/or sintering of iron.

In principle, since the FT catalyst is responsible for the syngas conversion, a similar CO conversion per unit weight of FT catalyst should be expected for all mixtures. However, since the FT synthesis is a strongly exothermic reaction, heat transfer effects can appear. The CO conversion, as well as its variation with time-on-stream, were higher for the FTQ mixture than for the mixtures with molecular sieves (Fig. 7). This result might be attributed to the intervention of thermal effects, which were more marked in the case of the FTQ mixture due to a lower bed dilution efficiency of the quartz sand compared to the aluminophosphates. The great difference in particle density between quartz sand and the FT catalyst led to bed fractionating (visually observed). This phenomenon increases the probability for hot spots to be generated. A more homogeneous mixture was obtained using α-Al_2O_3, whose particle density is closer to that of the FT catalyst. Recent tests performed using SAPO-11, FAPO-11 and α-Al_2O_3 [18], under reaction conditions similar to the present ones, showed CO conversions similar or lower for the mixture with α-Al_2O_3. Concerning the differences in CO conversion between FTS-11 and FTS-5 mixtures, it is possible that reactions taking place on the acid sites of SAPO-5 and SAPO-11 could give rise to a different thermal balance, which could affect the behaviour of the FT catalyst.

The iron present in FAPO-5 and FAPO-11 showed some degree of participation in the CO hydrogenation, since the conversions with the FTF-5 and FTF-11 mixtures were higher compared to that of the mixtures with SAPOs (Fig. 7). Besides, the CO conversion over FAPO-5 and FAPO-11 [18] seems to be lower when they are used alone than when they are mixed with the FT catalyst. The reaction environment differs in the two cases: the second one involves a higher concentration of water and hydrocarbons due to the higher-syngas conversion. Since aluminophosphate molecular sieves are susceptible to undergo structural changes by hydrothermal treatment, it would be possible for the catalytic properties of FAPOs to be modified under the reaction. Moreover, the difference in CO conversion (Fig. 7, see 2 days on stream) between the FT catalyst physically mixed with FAPO-11 and SAPO-11 was higher (15%) than between the FTF-5 and FTS-5 mixtures (8%). These results indicate that the syngas conversion was higher for FAPO-11 than for FAPO-5 under the environment originated with the physically mixed FT catalyst. Differences in thermal and hydrothermal stability of iron in these two structures could be involved. The stability of the framework iron in FAPO-11 could be lower than in FAPO-5; thus a higher proportion of iron in the former could undergo reduction and carburisation, with a consequently higher activity for CO hydrogenation. The increase of the FAPO-5 proportion from 1 to 2 (Fig. 8a) decreased the CO conversion suggesting that in this case the bed dilution effect for the FT catalyst was more important than the participation of iron in FAPO-5.

3.2.2.1. Mixtures with AFI molecular sieves. Significant differences on product selectivities after 2 h on stream were observed in the presence of FAPO-5 and SAPO-5 molecular sieves. The C_1–C_7

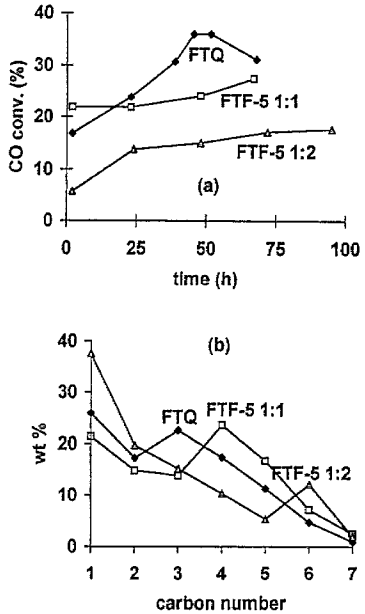

Fig. 8. Effect of the proportion of FAPO-5 mixed with FT catalyst. (a) CO conversion vs. time-on-stream; and (b) C_1–C_7 hydrocarbon distribution after 2 h on stream (573 K, 1.2 MPa, $H_2/CO=1$, 1.2 l/g_{FT} h).

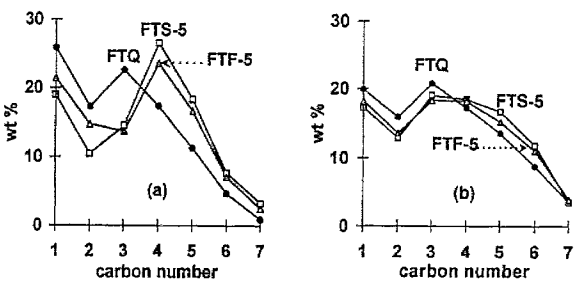

Fig. 9. C_1–C_7 hydrocarbon distribution for CO hydrogenation on the FT catalyst physically mixed with quartz sand and with AFI molecular sieves. (a) After 2 h; and (b) after 2 days on stream (573 K, 1.2 MPa, $H_2/CO=1$, 1.2 l/g_{FT} h, FT : quartz sand or molecular sieve 1 : 1).

hydrocarbon distribution (Fig. 9a, basis: 100% of C_1–C_7 hydrocarbons) showed a decrease in the C_3 fraction together with an increase of C_4 and C_5 hydrocarbons respect to the FTQ mixture. This tendency is similar to that shown by FAPO-5 alone (Fig. 6).

The alkenes/alkanes ratios after 2 h on stream for the C_{3+} fractions (Fig. 10) were much lower on FTF-5 and FTS-5 mixtures that on FTQ. As mentioned

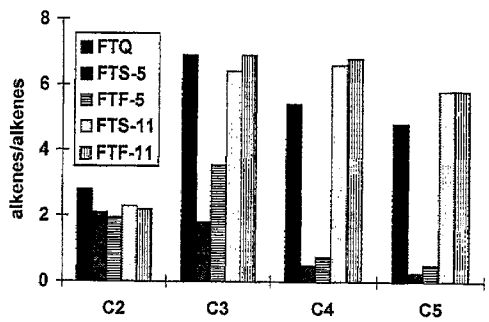

Fig. 10. Alkenes/alkanes ratios of the C_2–C_5 fractions for CO hydrogenation on the FT catalyst physically mixed with quartz sand and with AFI and AEL molecular sieves (573 K, 1.2 MPa, $H_2/CO=1$, 1.2 l/g_{FT} h, FT : quartz sand or molecular sieve 1 : 1, 2 h on stream).

before, propylene was transformed on acid sites giving rise to low propylene/propane ratios and to a decrease of the C_3 fraction. This was not the case for C_4 and C_5 hydrocarbons, which showed low alkenes/alkanes ratios, but they were present in high proportions (Fig. 9a). Hydrogen transfer reactions leading to more alkanes on the lighter fractions could account for this fact. Besides, iso-alkane/*n*-alkanes ratios for C_4 and C_5 fractions were much higher in the presence of FAPO-5 and SAPO-5 (Fig. 11a). These results suggest that alkenes formed on the FT catalyst underwent secondary reactions such as: oligomerisation; cracking; skeletal isomerisation; and hydrogen transfer in the presence of AFI molecular sieves. The increase of the FAPO-5 proportion in the mixture shifted the maximum from C_4 to C_6 hydrocarbons (Fig. 8b), most likely because of a higher density of acid sites and consequently more extensive secondary reactions.

The acid sites in FAPO-5 and SAPO-5 deactivated, mainly during the first day on stream. With increasing times-on-stream, the C_1–C_7 distribution (Fig. 9b), alkenes/alkanes and iso-/*n*-hydrocarbons ratios (Fig. 11b) approached to that of the FT catalyst alone.

3.2.2.2. Mixtures with AEL molecular sieves. Contrary to that observed for the mixtures with AFI sieves, the FTF-11 and FTS-11 mixtures did not show large changes on the C_1–C_7 hydrocarbon distribution (Fig. 12) compared to the FTQ mixture, except for the C_2–C_4 fraction on FTF-11. In the presence of FAPO-11, lower methane and higher C_2 and C_3 proportions were obtained. These results could be attributed to the

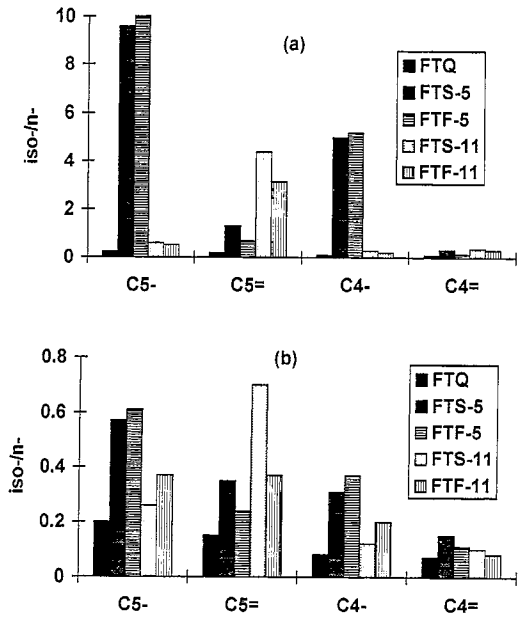

Fig. 11. Iso/normal ratios for C_5 and C_4 alkanes and alkenes for CO hydrogenation on the FT catalyst physically mixed with quartz sand and with AFI and AEL molecular sieves. (a) After 2 h; and (b) after 2 days on stream (573 K, 1.2 MPa, $H_2/CO=1$, 1.2 $l/g_{FT}.h$, FT : quartz sand or molecular sieve 1 : 1).

participation of the iron in FAPO-11 in CO hydrogenation forming light hydrocarbons with high selectivity.

AEL molecular sieves favoured skeletal isomerisation of alkenes, as seen for the C_5 fraction after 2 h on stream (Fig. 11a). The iso-pentenes/*n*-pentenes ratio progressively decreased becoming closer to that of the FTQ mixture (Fig. 11b). The differences introduced by these molecular sieves were greater for the C_5 than for the C_4 fraction. It is well known that alkenes reactivity on acid catalysis increases with increasing carbon number. More significant changes could be expected over the heavier fractions for longer times on stream.

Double bond shift reaction occurs readily over molecular sieves. Therefore, the mixture FTQ produced 1-alkenes with high selectivity, but in the presence of aluminophosphates the proportions of *cis* and *trans* internal alkenes were higher.

Selectivity showed to be more dependent on the structure (AFI or AEL) than on the element (Fe or Si) present in the aluminophosphate. Resemblance in product selectivities for the mixtures with molecular sieves of same structure, and significant differences between AFI and AEL structures were observed (Figs. 9–12). Although a comparison of selectivity should be made at the same conversion, the slight differences in CO conversion in this case did not have a major influence on the selectivity trends. Thus, regarding the catalytic behaviour for the first 2 h on stream when acid sites were less deactivated, CO conversion was slightly different (Fig. 7) for the mixtures with SAPO-5 and FAPO-5 (same structure, different element) but selectivity was very similar (Fig. 9a, Figs. 10 and 11a). On the other hand, CO conversion was closer for the mixtures with SAPO-11 and SAPO-5 (same element, different structure) but selectivity was quite different (Fig. 9a vs. Fig. 12a, Fig. 10 and Fig. 11a). The changes on product selectivity of the FT catalyst were more marked in the presence of FAPO-5 and SAPO-5 than with FAPO-11 and SAPO-11 molecular sieves. This could be related to a higher acidity and/or to lower restrictions by shape selectivity for AFI compared to AEL molecular sieves.

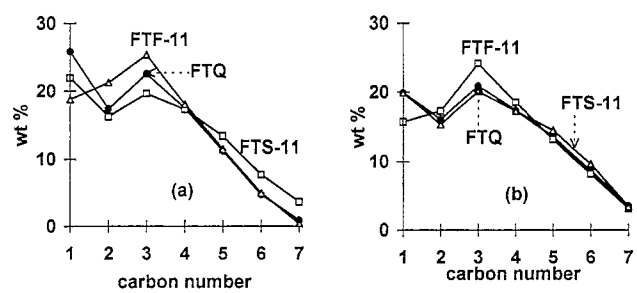

Fig. 12. C_1–C_7 hydrocarbon distribution for CO hydrogenation on the FT catalyst physically mixed with quartz sand and AEL molecular sieves (a) After 2 h; and (b) after 2 days on stream (573 K, 1.2 MPa, $H_2/CO=1$, 1.2 l/g_{FT} h, FT : quartz sand or molecular sieve 1 : 1).

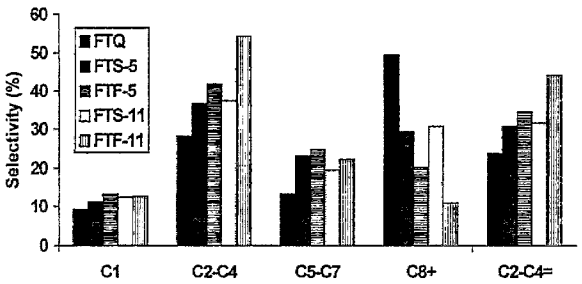

Fig. 13. Selectivities CO_2 free for CO hydrogenation with the FT catalyst physically mixed with quartz sand and AFI and AEL molecular sieves (573 K, 1.2 MPa, $H_2/CO=1$, 1.2 l/(g_{FT} h), FT : quartz sand or molecular sieve 1 : 1, 2 days on stream).

3.2.2.3. Hydrocarbons selectivity. The CO_2 selectivities were between 40 and 48% depending on conversion. Fig. 13 shows CO_2 free selectivities (carbon converted to a given fraction/total carbon converted to products different from CO_2) obtained after 2 days on stream. Selectivities to C_1–C_7 hydrocarbons were higher in the presence of all molecular sieves. This tendency, which has been reported previously in a patent for mixtures of a FT catalyst with SAPO-11 [19] remained during the tests (4 days). The increase in lighter hydrocarbon selectivities in the presence of the aluminophosphate sieves could be the combined result of several effects:

- dehydration of alcohols formed on the FT catalyst;
- cracking of heavy hydrocarbons; and
- interception of alkenes on acid sites.

Alkenes can participate in secondary reactions on FT sites, such as readsorption and chain growth [20]. Oxygenates can also be formed from alkenes, hydroformylation is an example. Since aluminophosphate sieves can intercept alkenes, these reactions would be suppressed when they are mixed with the FT catalyst, leading to an increase of the proportion of light hydrocarbons.

^{13}C NMR spectra of the liquid phase produced with mixtures of a FT catalyst with AEL molecular sieves [18] confirmed that the formation of oxygenated products (alcohols and carbonyl compounds) was lowered in the presence of these molecular sieves. A greater hydrocarbon variety, which included branched hydrocarbons, was also detected. This behaviour has been reported previously in the presence of SAPO-11 [19]. In addition, high-molecular weight hydrocarbons (waxes) observed at the reactor exit with the FTQ mixture were absent in the presence of aluminophosphates. This effect of decreasing high-molecular weight hydrocarbons without a great increase on methane formation can be advantageous to achieve high selectivities for fuels formation.

The highest selectivity to the C_2–C_4 fraction (both total and to alkenes, Fig. 13) was obtained for the mixtures with FAPOs, being higher for the FAPO-11. Again, the participation of a highly dispersed iron from FAPOs could be invoked. The potential of FAPOs as catalysts for syngas conversion is a subject which should further be explored.

4. Conclusions

Very different catalytic behaviours in syngas conversion were obtained for MeAPOs and Me/$AlPO_4$-5 with Me being iron and cobalt. The activity of iron-based catalysts FAPO-5 and Fe/$AlPO_4$-5 was low. The aqueous impregnation of $AlPO_4$-5 with iron led to a considerable decrease in surface area and support crystallinity as well as the reduction of iron became difficult on this catalyst. Iron in FAPO-5 remained mainly in the ionic state after the reduction–carburisation pre-treatment and syngas reaction. Acidic properties, which favour interception and conversion of alkenes produced by CO hydrogenation were evident for FAPO-5. The much higher syngas conversion activity and methane/C_3 ratio for Co/$AlPO_4$-5 compared to CoAPO-5 and CoAPO-34 could be associated with a higher metallic cobalt proportion for the former. On the other hand, the differences in product distribution observed between CoAPOs and FAPO-5 could be a consequence of the different alkenes selectivity of this metal-aluminophosphates molecular sieves.

The mixture of an iron-based FT catalyst with AFI and AEL molecular sieves containing iron and silicon modified the product distribution obtained by CO hydrogenation. Changes in product selectivity related to the acidic function were more dependent on the structural type than on the composition. In the presence of AFI molecular sieves alkenes formed on the FT catalyst underwent secondary reactions such as: oligomerisation; cracking; skeletal isomerisation; and hydrogen transfer. With AEL molecular sieves skeletal and double bond shift isomerisation were favoured.

Analysis of the lighter hydrocarbon fraction revealed that deactivation of acid sites with time-on-stream occurred. However, the relative proportion of lighter hydrocarbons remained higher when the sieves were present. Iron in FAPOs seems to participate in CO transformation, and the mixture of the iron FT catalyst with FAPO-11 gave rise to a higher selectivity to C_2–C_4 alkenes.

Acknowledgements

The authors want to thank to the Scientific and Humanistic Council of the Central University of Venezuela (CDCH-UCV) for financial support.

References

[1] C.H. Bartholomew, in: L. Guczi (Ed.), New Trends in CO Activation, (Studies in Surface Science and Catalysis, Vol. 64), Elsevier, Amsterdam, 1991, p. 158.
[2] V. Udaya, S. Rao, R.J. Gormley, Catal. Today 6 (1990) 207.
[3] D. Das, G. Ravichandran, D.K. Chakrabarty, S.N. Piramanayagan, S.N. Shringi, Appl. Catal. A 107 (1993) 73.
[4] J. G Ulan, R. Gronsky, R. Szostak, Zeolites 11 (1991) 466.
[5] M.R. Goldwasser, F. Navas, M.J. Pérez Zurita, M.L. Cubeiro, E. Lujano, C. Franco, F. González-Jiménez, E. Jaimes, D. Moronta, Appl. Catal. A 100 (1993) 85.
[6] R. Oukaci, J.C. S Wu, J.G. Goodwin Jr., J. Catal 110 (1988) 47.
[7] D. Arias, I. Campos, D. Escalante, J. Goldwasser, C.M. López, F. Machado, B. Méndez, D. Moronta, M. Pinto, V. Sazo, M.M. Ramírez de Agudelo, J. Mol. Catal. A 122 (1997) 175.
[8] B.M. Lok, C.A. Messina, R.L. Patton, R.T. Gajek, T.R. Cannan, E.M. Flanigen, U.S. Patent 4,440,871, 1984.
[9] C.A. Messina, B.M. Lok, E.M. Flanigen, US Patent 4,544,143 (1985).
[10] M. Alfonzo, J. Goldwasser, C.M. López, F.J. Machado, M. Matjhusin, B. Méndez, M.M. Ramírez de Agudelo, J. Mol. Catal. A 98 (1995) 35.
[11] C. Urbina de N., F. Machado, M. López, D. Maspero, J. Pérez-Pariente, Zeolites, 15 (1995) 157.
[12] C.M. López, C. Urbina, D. Máspero, F. Machado, J. Pérez-Pariente, Proceedings XIII Iberoam. Symp. Catal., vol 2, 1992, p. 1035.
[13] J. Ma, B. Fan, R. Li, J. Cao, Catal. Letters 23 (1994) 189.
[14] S.J. Jong, S. Cheng, Appl. Catal. A 126 (1995) 51.
[15] X. Song, A. Sayari, Appl. Catal. A 110 (1994) 121.
[16] D.B. Bukur, L. Nowicki, R.K. Manne, X. Lang, J. Catal. 155 (1995) 366.
[17] M.L. Cubeiro, M.R. Goldwasser, M.J. Pérez Zurita, C. Franco, F. González-Jiménez, E. Jaimes, Hyperfine Interact. 93 (1994) 1831.
[18] M.L. Cubeiro, C.M. López, F. Alvarez, in preparation.
[19] P.K. Coughlin, J.A. Rabo, US Patent 4,617,320 (1986).
[20] R.J. Madon, E. Iglesia, J. Catal. 139 (1993) 576.